

Dynamic Multiscaling of the Reaction-Diffusion Front for $mA + nB \rightarrow 0$.

Stephen Cornell,^{1,*} Zbigniew Koza,² and Michel Droz¹

¹*Département de Physique Théorique, Université de Genève, 24 quai Ernest-Ansermet, CH-1211
Genève 4, Switzerland.*

²*Institute of Theoretical Physics, University of Wrocław, pl. Maxa Born'a 9, PL-50-204 Wrocław,
Poland.*

(Preprint cond-mat/9412044: 9th December 1994)

Abstract

We consider the reaction zone that grows between separated regions of diffusing species A and B that react according to $mA + nB \rightarrow 0$, within the framework of the mean-fieldlike reaction-diffusion equations. For distances from the centre of the reaction zone much smaller than the diffusion length $X_D \equiv \sqrt{Dt}$, the particle density profiles are described by the scaling forms predicted by a quasistatic approximation, whereas they have a diffusive cut-off at a distance of order X_D . This cutoff, and the power-law decay of the quasistatic profiles, give rise to multiscaling behaviour, with anomalous values for the exponents describing the moments of the density and reaction profiles. Numerical solutions of the reaction-diffusion equations are in good quantitative agreement with the predictions of this theory.

PACS numbers: 82.40.-g, 82.30.-b, 02.30.Jr, 02.70.Bf

I. INTRODUCTION

The problem of a front that grows between initially separate regions of diffusing species A and B that react according to $mA + nB \rightarrow 0$ has provoked much recent interest [1–9]. Studies have concentrated on the scaling properties of the reaction rate R per unit volume and particle density profiles a and b , and on the critical dimension above which the mean-fieldlike reaction-diffusion rate equations are valid. In geometries where the only spatial variation of the densities is along the x -axis, these equations take the form [1,5]

$$\partial_t a = D\partial_x^2 a - mka^m b^n, \quad (1)$$

$$\partial_t b = D\partial_x^2 b - nka^m b^n, \quad (2)$$

where k is the reaction constant, and here and subsequently the reagents are assumed to have the same diffusion constant D . The initial conditions appropriate to this problem are

$$a(x, 0) = a_0\theta(x), \quad (3)$$

$$b(x, 0) = b_0\theta(-x), \quad (4)$$

where a_0 and b_0 are constants, and θ is the Heavyside function. The quantity $u \equiv (a/m - b/n)$ obeys a simple diffusion equation, with solution [5]

$$u = \frac{1}{2} \left(\frac{a_0}{m} - \frac{b_0}{n} \right) - \frac{1}{2} \left(\frac{a_0}{m} + \frac{b_0}{n} \right) \operatorname{erf} \left(\frac{x}{2\sqrt{Dt}} \right). \quad (5)$$

The reaction is concentrated in the region where the densities of the two species are comparable. The centre x_f of the reaction zone may be defined as the point where $u = 0$. We therefore have

$$x_f = 2(Dt)^{1/2} \operatorname{erf}^{-1} \left[\frac{(a_0/m - b_0/n)}{(a_0/m + b_0/n)} \right], \quad (6)$$

so if $a_0/m = b_0/n$ we have $x_f = 0$ (n.b. in reference [5], x_f was defined as the point of maximal reaction, which is not necessarily the same point).

If one assumes that the penetration of one species into the other is much shallower than the diffusion length $(Dt)^{1/2}$, the reaction between the two species takes place within a distance $w \ll (Dt)^{1/2}$ of x_f . One expects that, for $x \ll (Dt)^{1/2}$, the profiles will be described by the single lengthscale w , leading to the following scaling hypothesis [1,5]

$$a(x, t) = t^{-\gamma} A \left(\frac{x - x_f}{t^\alpha} \right), \quad (7)$$

$$b(x, t) = t^{-\gamma} B \left(\frac{x - x_f}{t^\alpha} \right), \quad (8)$$

$$R(x, t) = t^{-\beta} \phi \left(\frac{x - x_f}{t^\alpha} \right), \quad (9)$$

where $w \sim t^\alpha$, $\phi = A^m B^n$, and $\beta = (m + n)\gamma$. The number of particles of either species arriving at the reaction front is $\propto t^{-1/2}$, which must equal the total reaction rate, so we

must have $\beta - \alpha = 1/2$. Consistency of this scaling ansatz with the equations of motion leads to $\alpha = (1/2)(m + n - 1)/(m + n + 1)$ [5].

The related case of a front formed by opposing constant diffusion currents $J_A = mJ$ and $J_B = -nJ$ of A - and B -particles imposed at $x = -\infty$ and $+\infty$ respectively has recently been studied [10–12]. In this case, the system approaches a steady state where the equations

$$(D/m)\partial_x^2 a = ka^m b^n = (D/n)\partial_x^2 b, \quad (10)$$

and boundary conditions may be written in dimensionless form, so that the following scaling ansatz is valid for all x [11]:

$$R(x) = \frac{J}{w}\phi_{ss}\left(\frac{x}{w}\right), \quad (11)$$

$$a(x) = JwA_{ss}\left(\frac{x}{w}\right), \quad (12)$$

$$b(x) = JwB_{ss}\left(\frac{x}{w}\right), \quad (13)$$

where $w(J, D, k) \propto J^{-\nu}$ and $\nu = (m + n - 1)/(m + n + 1)$. From (10), we have $\partial_x^2 u = 0$ [$u \equiv (a/m - b/n)$], whose solution with these boundary conditions is $u = -Jx/D$. For $(x/w) \gg 1$, the B -particles are overwhelmingly in the majority, so one has $b = nJx/D + na/m \approx nJx/D$, and hence $A''_{ss}(y) \sim (A_{ss})^m y^n$, leading to

$$A_{ss}(y) \sim \begin{cases} y^{-n/4} \exp(-\sigma y^{1+(n/2)}) & \text{for } m = 1, \\ y^{-(n+2)/(m-1)} & \text{for } m > 1, \end{cases} \quad (14)$$

as $y \rightarrow \infty$, where σ is a constant. Similar results hold for B_{ss} by interchanging m and n . Within this approach, it is also possible to show [11] that the ‘mean-field’ assumption $R = ka^m b^n$ (assumed in all the above equations) is valid for microscopic stochastic systems in spatial dimension $d > d_c \equiv 2/(m + n - 1)$.

For the time-dependent problem, when $x \gg w$ one of the species is overwhelmingly in the majority, so $|u| \rightarrow \max(a/m, b/n)$, and the profile of the majority particle density is $\sim |x - x_f|/t^{1/2}$ for $(Dt)^{1/2} \gg x \gg w$. The diffusion current of particles arriving at x_f is therefore $J \sim t^{-1/2}$, and the characteristic timescale on which this current changes is $(d \log J/dt)^{-1} \propto t$. The equilibration time of the front is of order Dw^2 , so since $\alpha < 1/2$ one would expect that the reaction zone has enough time to reach the steady-state profile it would have if the current J were constant. One would therefore predict that the results of the steady-state problem, and hence the dynamic scaling ansatz, would be applicable to the time dependent case for $x \ll (Dt)^{1/2}$ [11].

For $m = n = 1$ the scaling forms (7–9) have been proved rigorously to describe the asymptotic behaviour as $t \rightarrow \infty$ of the reaction-diffusion equations (1,2) [7]. Experiments on real systems, and simulations of microscopic stochastic models, also appear to verify the scaling theory and exponents in dimension $d \geq 2$ [2–4]. For $d = 1$, there has been some controversy as to whether the scaling theory is valid [5,8], but the most recent results [9] appear to show that the steady-state results do indeed apply. However, for $(m, n) \neq (1, 1)$, where rigorous mathematical results are not available, the case is much less clear. Numerical simulations of microscopic stochastic models in $d = 1$ are consistent with a scaling ansatz

[6], but they are of low precision, since reaction events are much rarer than for $m = n = 1$. The fact that at least one of the particle density profiles must decay algebraically (see Eq. (14)) might invalidate the assumption that reactions take place within a zone of width $w \ll (Dt)^{1/2}$.

In this paper, we shall give careful arguments to show that the scaling ansatz is indeed valid for lengthscales much smaller than $\sim t^{1/2}$. We shall then show that the two lengthscales in the problem, w and $(Dt)^{1/2}$, together with the power law tails of the steady-state profile, give rise to a multiscaling form for the particle density profile, whose moments are described by a spectrum of exponents between α and $1/2$. We then present numerical solutions of the reaction-diffusion equations, and show that the results are in good agreement with the theoretical predictions.

II. VALIDITY OF THE SCALING ANSATZ

The scaling ansatz can be shown to be exact for the case of a steady-state front formed between balancing opposing currents, and so its applicability to the time-dependent case relies on the front being formed quasi-statically [11]. Naively, one would expect that the time for a diffusive system to equilibrate within a region of size $\sim t^\nu$ would be $\propto t^{2\nu}$, whereas the timescale upon which the current $J \propto t^{-1/2}$ changes is $(d \log J/dt)^{-1} \propto t$, which predicts that quasistatic approximation would be valid for lengthscales with $\nu < 1/2$. However, since some of the density profiles decay algebraically, one might wonder whether the flow of particles towards $|x| \rightarrow \infty$ necessary to sustain these steady-state profiles might be too great for the quasi-static approximation to be valid.

In this section, we shall show that the quasistatic approximation is internally consistent for lengthscales smaller than $t^{1/2}$, in that it predicts that: (i) the number of particles up to a distance $\sim t^{1/2}$ is always much less than the total particles that have reacted, so that the number of particles in the tails is never too much to have a feedback effect on the profiles at distances of order $t^{1/2}$; (ii) the time taken for each part of the particle density tail to equilibrate at its quasistatic value is always much less than the characteristic timescale on which this value changes. We shall then discuss what this implies about the behaviour of the moments of the density and reaction profiles.

Consider the part of the tail of the A -particle profile $a(x, t) \sim t^{-\gamma}(x/t^\alpha)^{-\lambda}$, where $\lambda = [n + 2]/[m - 1]$ (see Eq. (14)), in the region $x_1 < x < x_2$, with $x_1 \propto t^{\epsilon_1}$ and $x_2 \propto t^{\epsilon_2}$ ($\alpha < \epsilon_1 < \epsilon_2 < 1/2$). The current of A -particles at x is

$$J_A = -D\partial_x a \sim \frac{a(x, t)}{x}, \quad (15)$$

so the ratio $J_A(x_2)/J_A(x_1) = t^{-(\epsilon_2 - \epsilon_1)(1 + \lambda)} \rightarrow 0$ as $t \rightarrow \infty$. Almost all of the particles that enter at x_1 are therefore removed by the reaction, rather than by diffusing out at x_2 . The number of particles in the region is

$$N_A \equiv \int_{x_1}^{x_2} a dx \sim \begin{cases} a(x_1)x_1 & \text{for } \lambda > 1, \\ t^{\alpha - \gamma} \log\left(\frac{x_2}{x_1}\right) & \text{for } \lambda = 1, \\ a(x_2)x_2 & \text{for } \lambda < 1. \end{cases} \quad (16)$$

The number of particles in the tail can diverge for certain values of λ . This could invalidate the assumption that the total reaction rate equals the number of particles arriving at the origin if this number were found to be larger than the total number of particles $\propto t^{1/2}$ that have reacted. However, the total number of particles in the tail up to a lengthscale $t^{1/2}$, found by substituting $\epsilon_2 = 1/2$, is found in each of the above cases to be of order less than $t^{1/2}$. The time taken for N_A particles to enter the region $x_1 < x < x_2$ is

$$N_A/J_A(x_1) \sim \begin{cases} t^{2\epsilon_1} & \text{for } \lambda > 1, \\ t^{2\epsilon_1} \log t & \text{for } \lambda = 1, \\ t^{\epsilon_1 + \epsilon_2 - (\epsilon_2 - \epsilon_1)(1 - \lambda)} & \text{for } \lambda > 1, \end{cases} \quad (17)$$

which is always $\ll t$ since $\epsilon_1 < \epsilon_2 < 1/2$. The front therefore has enough time to reach its steady-state value for lengthscales smaller than $t^{1/2}$.

The scaling ansatz (7-9) would therefore appear to be consistent for all lengthscales $\sim t^\epsilon$, with $\epsilon < 1/2$. For $\epsilon \geq 1/2$, the density of particles is limited by diffusion, and so we expect there to be some kind of exponential cutoff in all of the profiles on such lengthscales. We therefore propose the following ansatz for a and b in the limit $t \rightarrow \infty$:

$$a(x, t) = a_{ss}(x, t)G_A\left(\frac{x}{t^{1/2}}\right), \quad (18)$$

$$b(x, t) = b_{ss}(x, t)G_B\left(\frac{x}{t^{1/2}}\right), \quad (19)$$

where $a_{ss} = t^{-\gamma}A_{ss}(x/t^\alpha)$ and $b_{ss} = t^{-\gamma}B_{ss}(x/t^\alpha)$ are the solutions to the steady-state equations (12,13), and $G_A(y)$ and $G_B(-y)$ are functions that provide a cutoff at $y = \mathcal{O}(1)$, and ensure that $a(x, t)$ and $b(x, t)$ satisfy (5) away from the reaction zone. The actual form of $G_A(y)$ and $G_B(-y)$ is unimportant, provided that all moments of the tail for $y > 0$ are defined and that there is no power-law behaviour for $y \rightarrow 0$.

This form leads to multiscaling behaviour for the moments of the particle profiles, by virtue of the power law tails of a and/or b when $(m, n) \neq (1, 1)$. Consider a function F of the form $F(x, t) = t^{-\delta}\phi(x/t^\alpha)G(x/t^{1/2})$, where $\phi(y) \rightarrow y^{-\mu}$ as $y \rightarrow \infty$, $\phi \rightarrow 1$ as $y \rightarrow 0$, $G(y) \rightarrow 1$ as $y \rightarrow 0$, and all positive moments of G are defined. Then the q 'th moment of F is of the form

$$\begin{aligned} \int_0^\infty x^q F(x, t) dx &= \int_0^\infty x^q t^{-\delta} \phi\left(\frac{x}{t^\alpha}\right) G\left(\frac{x}{t^{1/2}}\right) dx \\ &\sim \begin{cases} t^{\alpha(q+1)-\delta} & \text{for } \mu > q + 1, \\ t^{\alpha(q+1)-\delta} \log t & \text{for } \mu = q + 1, \\ t^{\alpha\mu - \delta + \frac{1}{2}(q - \mu + 1)} & \text{for } \mu < q + 1. \end{cases} \end{aligned}$$

When $\mu > q + 1$, the q 'th moment of ϕ is finite, whereas, for $\mu < q + 1$, the dominant contribution comes from $(x/t^{1/2}) = \mathcal{O}(1)$. Defining $X^{(q)} \equiv [\int x^q F dx / \int F dx]^{1/q}$, we find that, for $\mu \leq 1$, $X^{(q)} \sim t^{1/2}$ (with logarithmic corrections for $\mu = 1$). For $\mu < 1$, we find the multiscaling behaviour $X^{(q)} \sim t^{\zeta_q}$, with ζ_q increasing monotonically as a function of q from α to $1/2$.

By substituting from (14) the appropriate power-law tails of A_{ss} and B_{ss} , the multiscaling forms predict the following behaviour for the following quantities (without loss of generality, we have assumed $m \geq n$):

$$w^2 \equiv \frac{\int_{-\infty}^{\infty} x^2 R(x, t) dx}{\int_{-\infty}^{\infty} R(x, t) dx} \sim \begin{cases} t^{2\alpha} & \text{for } m - n < 3, \\ t^{2\alpha} \log t & \text{for } m - n = 3, \\ t^{1 - (\frac{1}{2} - \alpha)(\nu - 1)} & \text{for } m - n > 3, \end{cases} \quad (20)$$

$$w_a^2 \equiv \frac{\int_{-\infty}^{x_f} x^2 a(x, t) dx}{\int_{-\infty}^{x_f} a(x, t) dx} \sim \begin{cases} t^{2\alpha} & \text{for } 3m - n < 5, \\ t^{2\alpha} \log t & \text{for } 3m - n = 5, \\ t^{1 - (\frac{1}{2} - \alpha)(\lambda - 1)} & \text{for } 3m > n + 5 > m + 2, \\ \frac{t}{\log t} & \text{for } m - n = 3, \\ t & \text{for } m - n > 3, \end{cases} \quad (21)$$

$$w_b^2 \equiv \frac{\int_{x_f}^{\infty} x^2 b(x, t) dx}{\int_{x_f}^{\infty} b(x, t) dx} \sim \begin{cases} t^{2\alpha} & \text{for } m + 5 > 3n, \\ t^{2\alpha} \log t & \text{for } m + 5 = 3n, \\ t^{1 - (\frac{1}{2} - \alpha)(\kappa - 1)} & \text{for } m + 5 < 3n, \end{cases} \quad (22)$$

where $\lambda = (n + 2)/(m - 1)$, $\nu = 2 + \lambda$, and $\kappa = (m + 2)/(n - 1)$. If these quantities were described by a one-length scaling theory, all of these quantities would behave as $\sim t^{2\alpha}$, so we describe departure from this behaviour as ‘anomalous’.

Defining

$$x_c \equiv \frac{\int_{-\infty}^{\infty} x R(x, t) dx}{\int_{-\infty}^{\infty} R(x, t) dx}, \quad (23)$$

a similar procedure may be used to find the scaling behaviour for x_c . Notice, however, that the contribution to x_c coming from the scaling term is identically zero, since $mR_{ss} = D\partial_x^2 a$ implies $\int_{-\infty}^{\infty} x R_{ss} dx = 0$. The behaviour of x_c is therefore determined wholly by the corrections to scaling. From (1,2), one has

$$\int_{-\infty}^{\infty} x R dx = \int_{-\infty}^0 \frac{D}{m} x \partial_x^2 a dx + \int_0^{\infty} \frac{D}{n} x \partial_x^2 b dx - \int_{-\infty}^0 x \partial_t a dx - \int_0^{\infty} x \partial_t b dx. \quad (24)$$

The first two terms may be integrated by parts, yielding $D[a(0, t)/m - b(0, t)/n]$, which is zero by virtue of (5) for the initial conditions $u(0, 0) = 0$. The final two terms are of opposite sign, and cancel identically for $m = n$ by symmetry. For $m \neq n$, they typically have different scaling behaviours, and so the scaling behaviour is determined by the largest term. Substituting the forms (18,19) for a and b , and differentiating, one finds the following scaling behaviour for x_c .

$$x_c \sim \begin{cases} t^{3\alpha - 1} & \text{for } 2m - n < 4, \\ t^{\frac{1}{2} - \frac{1}{m-1}} \log t & \text{for } 2m - n = 4, \\ t^{\alpha - (\frac{1}{2} - \alpha)\lambda} & \text{for } 2m - n > 4. \end{cases} \quad (25)$$

III. NUMERICAL SIMULATIONS

In order to verify the scaling ansatz (7–9) we have solved the reaction-diffusion equations (1,2) numerically. We approximated (1) and (2) with a finite-difference method, with Δt , Δx satisfying $k\Delta t = 0.01$, $D\Delta t/(\Delta x)^2 = 0.04$, and a lattice of $N = 12001$ sites, which was sufficient for finite-size effects to be unimportant. Henceforth we will choose the reference system in which $\Delta x = \Delta t = 1$, so that our numerical results will correspond to the case $k = 0.01$ and $D = 0.04$. The initial condition satisfied $a_0/m = b_0/n$, so that $x_f = 0$ from (6). The reaction rate R thus obtained for times $t = 10^3 \dots 10^7$ and $n = 1, 2 \leq m \leq 4$ are presented in Figures 1–3, rescaled by $t^{\alpha+\frac{1}{2}}$ and plotted as a function of x/t^α . The solid curve in each figure is a numerical solution the steady-state equation (10), for the same values of D and k , and using the time dependent current as boundary condition. We see that the data appear to converge to the solid line as $t \rightarrow \infty$, so that the scaling ansatz (7–9) is valid in the sense that

$$t^{\alpha+\frac{1}{2}}R(x/t^\alpha) \rightarrow F(x/t^\alpha) \quad \text{as } t \rightarrow \infty, \quad (26)$$

where $F(x/t^\alpha)$ is a function of x/t^α . Notice that the convergence appears to be slower for larger values of m .

Another interesting feature of Figures 1–3 is that the point at which R reaches its maximal value differs from 0. As the x -axes of these figures have been rescaled by a factor t^α , the location of this point changes with time like t^α . This shows that the definition of x_f as the point of maximal reaction is not equivalent to the definition in this article as the point where $u = 0$.

To verify the multiscaling properties of the reaction zone, we investigated the behaviour of the functions w , w_a , w_b , and x_c . According to (20–23), they should diverge as $t^\nu \log^\kappa(t)$, with ν and κ being some exponents dependent on m and n . In Figs. 4–7 we have plotted these quantities, rescaled by $\log^{-\kappa} t$, on a log-log scale, using the theoretical values of κ . The values of ν_w , ν_a , ν_b , and ν_c (corresponding to the behaviour of the properties w , w_a , w_b , and x_c respectively) were estimated from a least-squares fit to the last decade in these figures, and are compared with the theoretical values in Table 1. Agreement for most of the exponents is very good. Since $n = 1$, the theory predicts that ν_b assumes its non-anomalous value α , and the measured values are in close agreement. The values for ν_a are anomalous, and are also well reproduced. The values for ν_w and ν_c are close to the theoretical predictions for $m = 2$, but deviate for $m = 3$ and 4.

The reason why some of the exponents deviate from the theoretical values may be understood from Figs. 1–3. The convergence to the solid curve for $x < 0$, where Eq. (14) predicts an exponential decay, is very rapid—semilog plots of $R(-x)$ were found to be in very good agreement with these predictions for up to 10 decades. However, the convergence of the profiles to the steady-state profiles is much slower for $x > 0$ (where the asymptotic behaviour is algebraic). In fact, numerical investigation of the steady-state profiles showed that the regime for which the power law behavior predicted by (14) appears is beyond the point at which the diffusive cutoff is already active in the data. This means that the asymptotic regime has not yet been reached. In view of this fact, the agreement between the measured exponents and the theory is surprisingly good.

IV. CONCLUSIONS

The multiscaling theory predicts that the reaction profile of the system is described asymptotically by a scaling form, in the sense that Eq. (26) holds, but that the moments of the reaction and density profiles may have anomalous behavior. Numerical solutions of the reaction-diffusion equations verify the asymptotic scaling behavior, and also give values for the anomalous exponents close to those predicted by the theory. Longer times would have to be simulated to find better values for the exponents.

The convergence to the asymptotic behavior becomes progressively slower as the order of the reaction is increased. This means that simulations probing the asymptotic behavior also become more difficult. Nevertheless, Eq. (20) suggests that it would be worthwhile to look at at least one case where $m - n > 3$.

In the steady-state problem, it has been shown [11] that the critical dimension is $d_c = 2/(m+n-1)$. This means that the reaction-diffusion equations correctly describe the scaling behavior of ‘real’ stochastic realizations for all physical dimensions, except for $(m, n) = (2, 1)$ in dimension 1, where logarithmic corrections to the steady-state behavior are expected. Because of the strong link between the steady-state problem and the time-dependent problem studied in the present article, we expect the critical dimensions to be the same. The only microscopic simulation results available [6] agree broadly with the picture in the present article, though they are not of sufficiently high quality to give a thorough test.

The theory outlined in this paper is based on heuristic arguments and numerical results only, so a first-principles analytical justification is needed. It would be possible to write the equation of motion for the corrections to the multiscaling terms, and then investigate whether they are truly small and do not contribute to the behavior of the moments. Although no conclusive results have been found, a preliminary attempt at this procedure suggests that there may be values for m and n where the assumption may break down that the interpenetration of the species is smaller than the number of particles that have reacted [13]. The multiscaling theory presented in this paper might therefore have to be revised in those cases.

ACKNOWLEDGEMENTS

ZK was supported by KBN Grant no. 2P 302 181 07. MD acknowledges support from the Swiss National Science Foundation. We would like to thank Peter Wittwer for stimulating discussions.

REFERENCES

- * Current Address: Department of Mathematics and Statistics, University of Guelph, Guelph, Ontario N1G 2W1, Canada.
- [1] L. Gálfi and Z. Rácz, Phys. Rev. A **38**, 3151 (1988).
 - [2] Z. Jiang and C. Ebner, Phys. Rev. A **42**, 7483 (1990).
 - [3] B. Chopard and M. Droz, Europhys. Lett. **15**, 459 (1991).
 - [4] Y.-E. Koo, L. Li, and R. Kopelman, Mol. Cryst. Liq. Cryst. **183**, 187 (1990); Y.-E. Koo and R. Kopelman, J. Stat. Phys. **65**, 893 (1991).
 - [5] S. Cornell, M. Droz, B. Chopard, Phys. Rev. A **44**, 4826 (1991).
 - [6] S. Cornell, M. Droz, B. Chopard, Physica **A188**, 322 (1992).
 - [7] A. Schenkel, J. Stubbe, P. Wittwer, Physica **D69**, 135 (1993).
 - [8] M. Araujo, H. Larralde, S. Havlin, and H.E. Stanley, Phys. Rev. Lett. **71**, 3592 (1993).
 - [9] S. Cornell, to appear in Phys. Rev. Lett. (1994); S. Cornell, to be published (1994).
 - [10] E. Ben-Naim and S. Redner, J. Phys. A **25**, L575 (1992).
 - [11] S. Cornell, M. Droz, Phys. Rev. Lett. **70**, 3824 (1993).
 - [12] B. Lee and J. Cardy, Phys. Rev. E **50** 3287 (1994).
 - [13] P. Wittwer, private communication.

TABLES

TABLE I. The measured values of the exponents ν_w , ν_a and ν_b describing w , w_a , w_b and x_c respectively, together with the non-anomalous exponent α , for three values of the duple (m, n) . The values in square brackets are the predictions of the multiscaling theory; the presence of a value for κ indicates the presence of a logarithmic correction of the form $\log^\kappa(t)$, account of which has been taken in calculating the ν .

| Quantity | (2,1) | (3,1) | (4,1) |
|----------|--|-----------------------|---|
| α | $\frac{1}{4}$ | $\frac{3}{10}$ | $\frac{1}{3}$ |
| ν_w | 0.26 $[\frac{1}{4}]$ | 0.35 $[\frac{3}{10}]$ | 0.37 $[\frac{1}{3}, \kappa = \frac{1}{2}]$ |
| ν_a | 0.27 $[\frac{1}{4}, \kappa = \frac{1}{2}]$ | 0.44 $[0.45]$ | 0.50 $[\frac{1}{2}, \kappa = -\frac{1}{2}]$ |
| ν_b | 0.25 $[\frac{1}{4}]$ | 0.29 $[\frac{3}{10}]$ | 0.32 $[\frac{1}{3}]$ |
| ν_c | -0.25 $[-\frac{1}{4}]$ | 0.06 $[0]$ | 0.21 $[\frac{1}{6}]$ |

FIGURES

FIG. 1. $R \cdot t^\beta$ vs. x/t^α for $n = 1$ and $m = 2$ and $t = 10^3, 10^4, \dots, 10^7$.

FIG. 2. $R \cdot t^\beta$ vs. x/t^α for $n = 1$ and $m = 3$ and $t = 10^3, 10^4, \dots, 10^7$.

FIG. 3. $R \cdot t^\beta$ vs. x/t^α for $n = 1$ and $m = 4$ and $t = 10^3, 10^4, \dots, 10^7$.

FIG. 4. Log-log plot of $w \log^{-\kappa}(t)$ versus t . The straight lines are a least-squares fit to the last decade.

FIG. 5. Log-log plot of $w_a \log^{-\kappa}(t)$ versus t . The straight lines are a least-squares fit to the last decade.

FIG. 6. Log-log plot of $w_b \log^{-\kappa}(t)$ versus t . The straight lines are a least-squares fit to the last decade.

FIG. 7. Log-log plot of $x_c \log^{-\kappa}(t)$ versus t . The straight lines are a least-squares fit to the last decade.

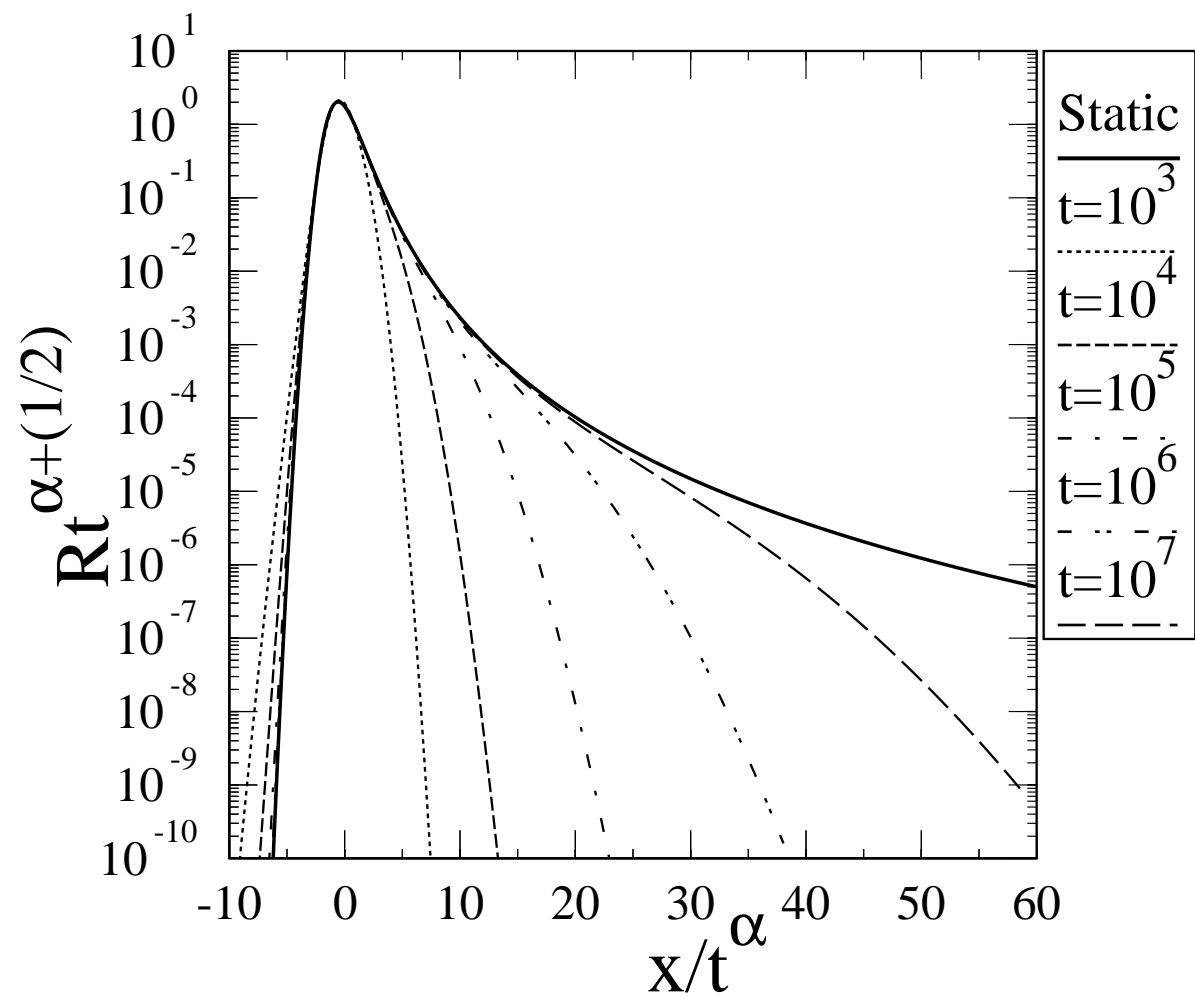


Figure 1

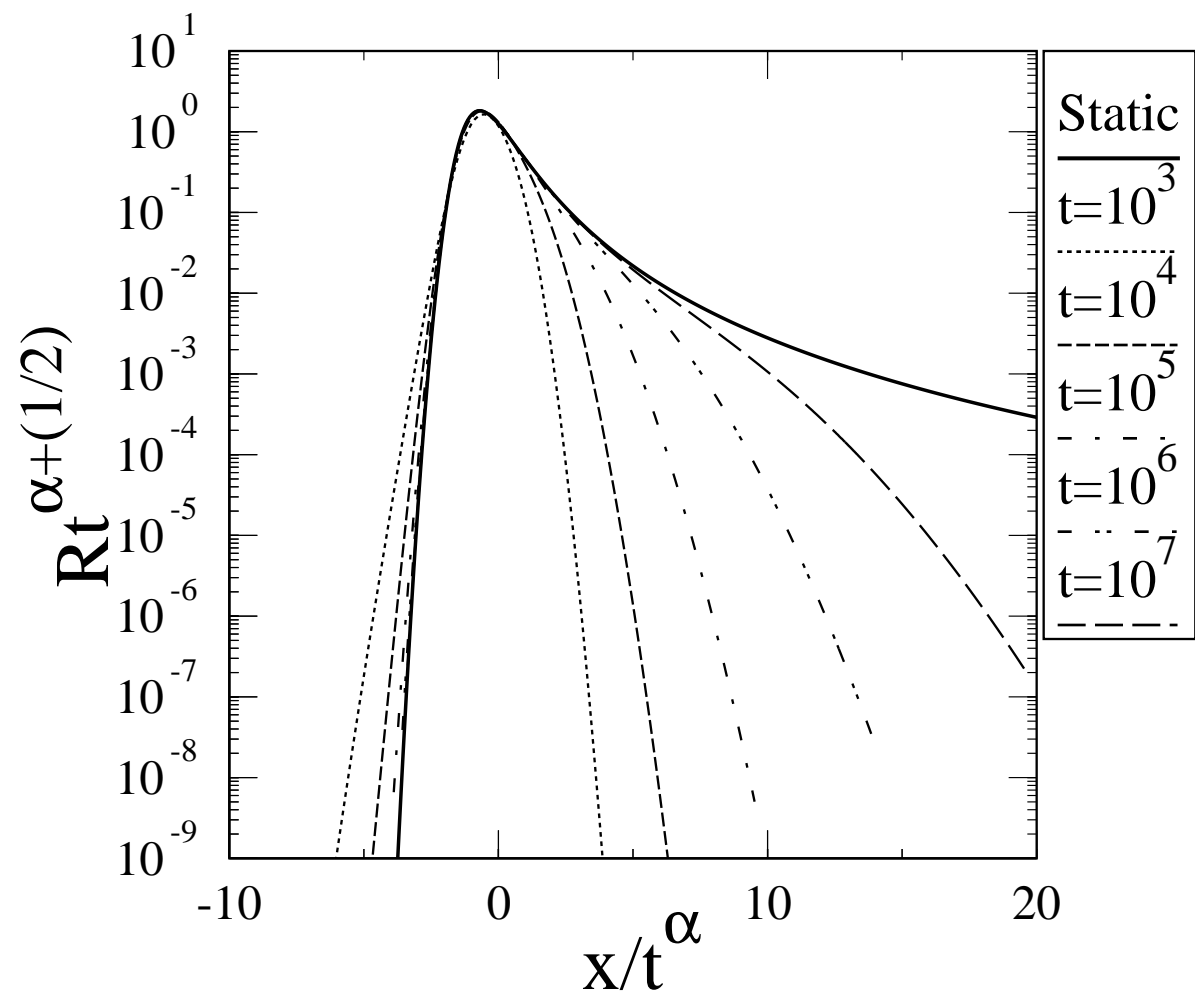


Figure 2

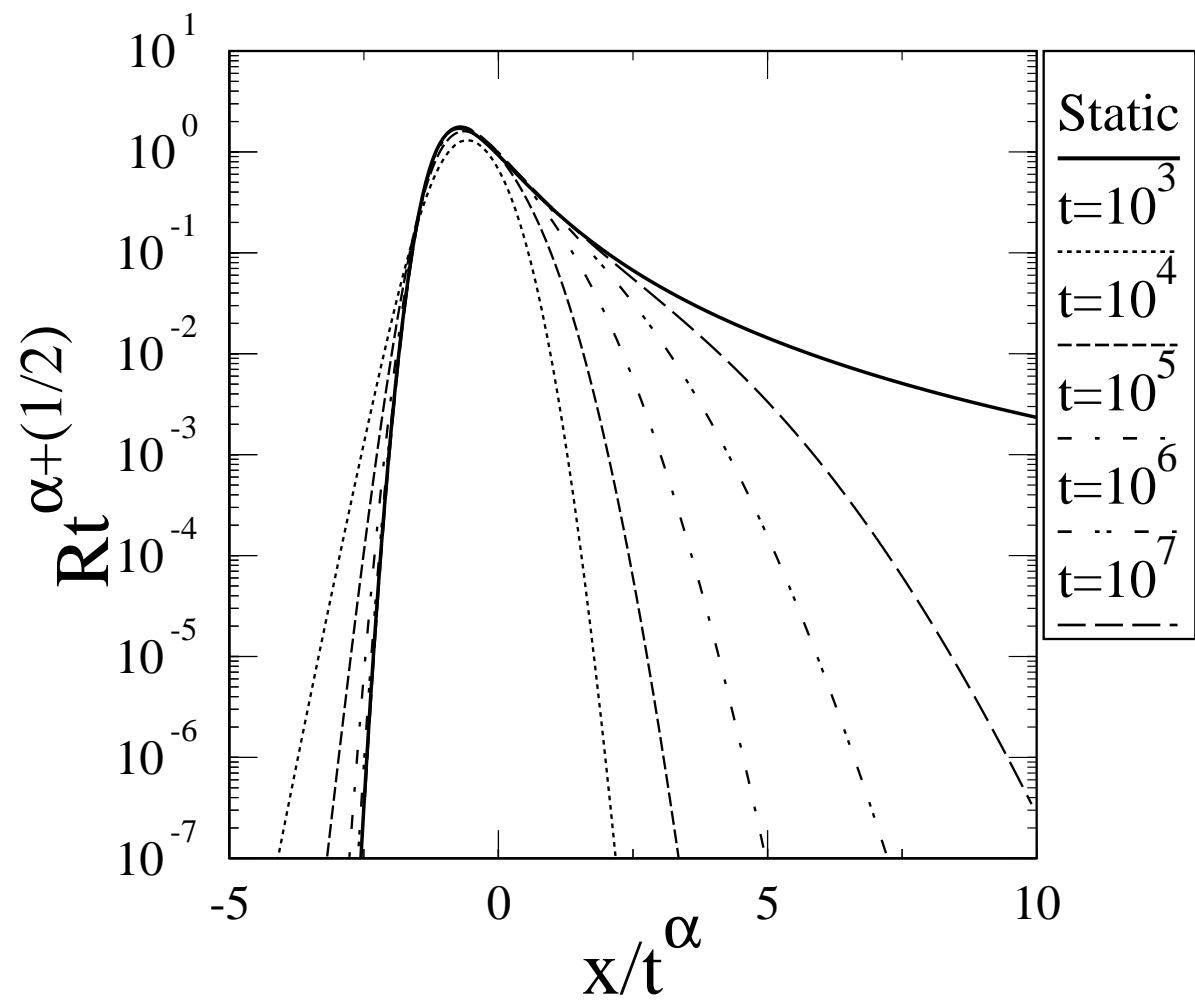


Figure 3

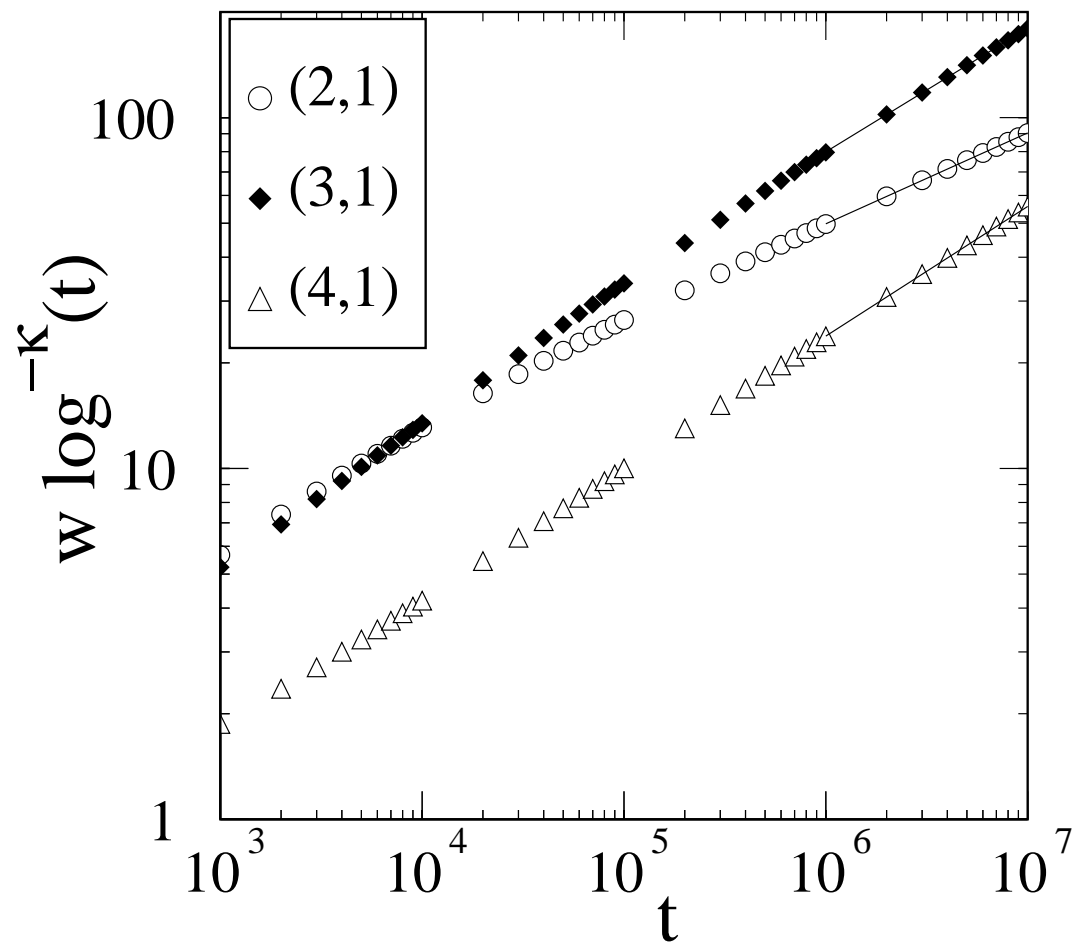


Figure 4

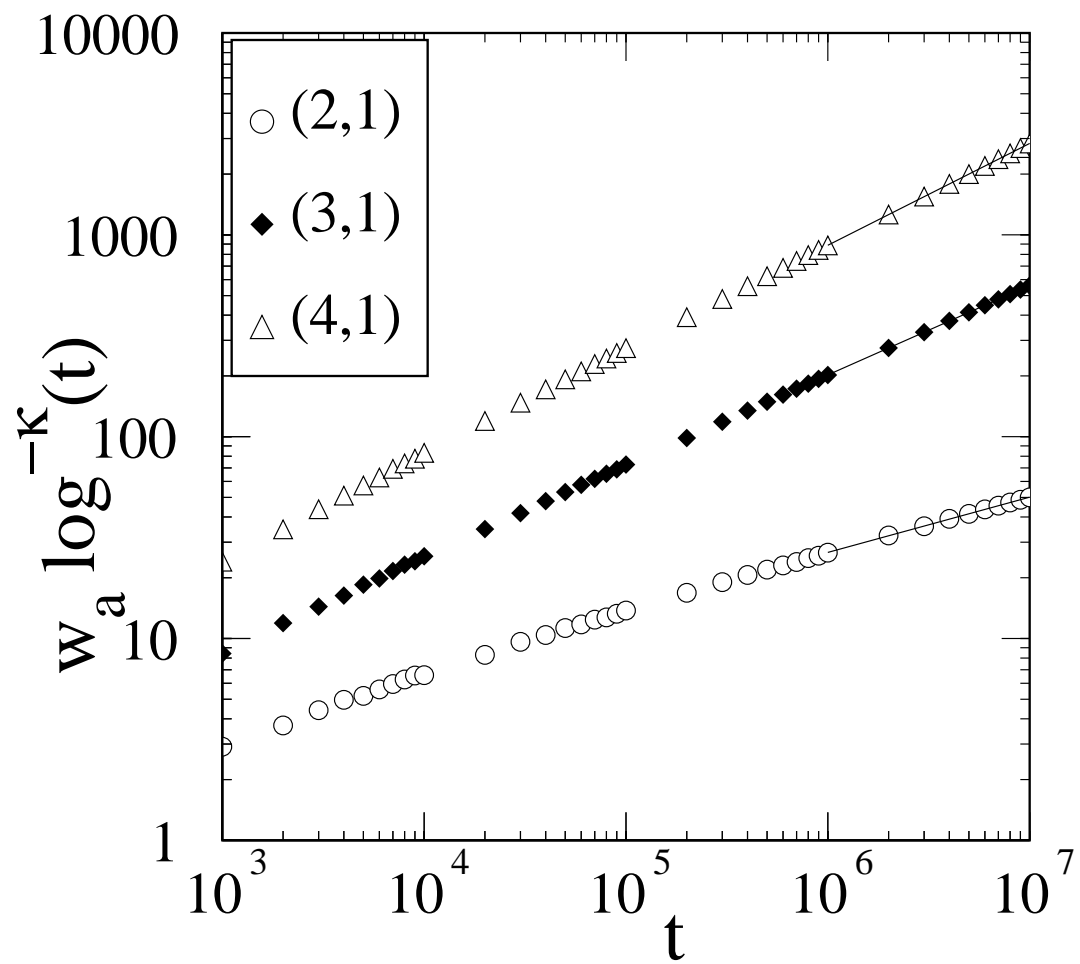


Figure 5

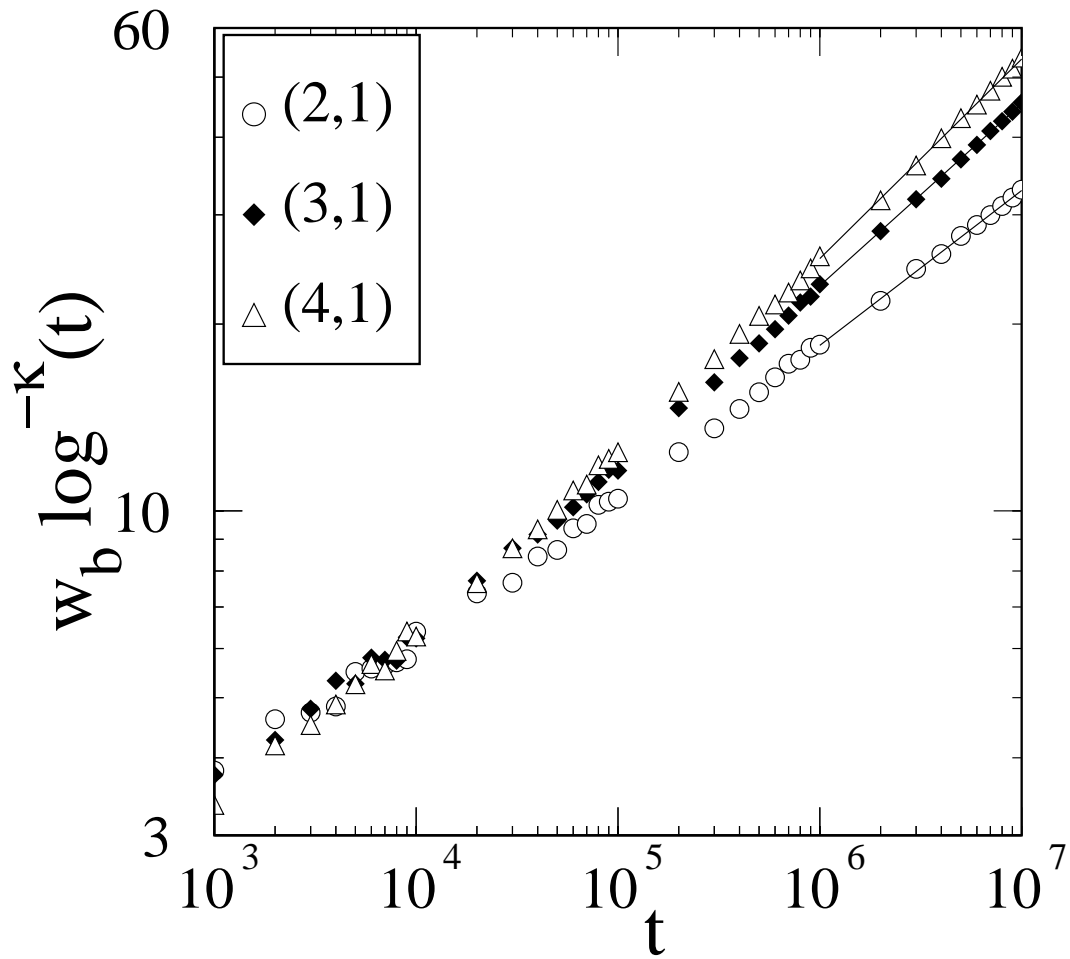


Figure 6

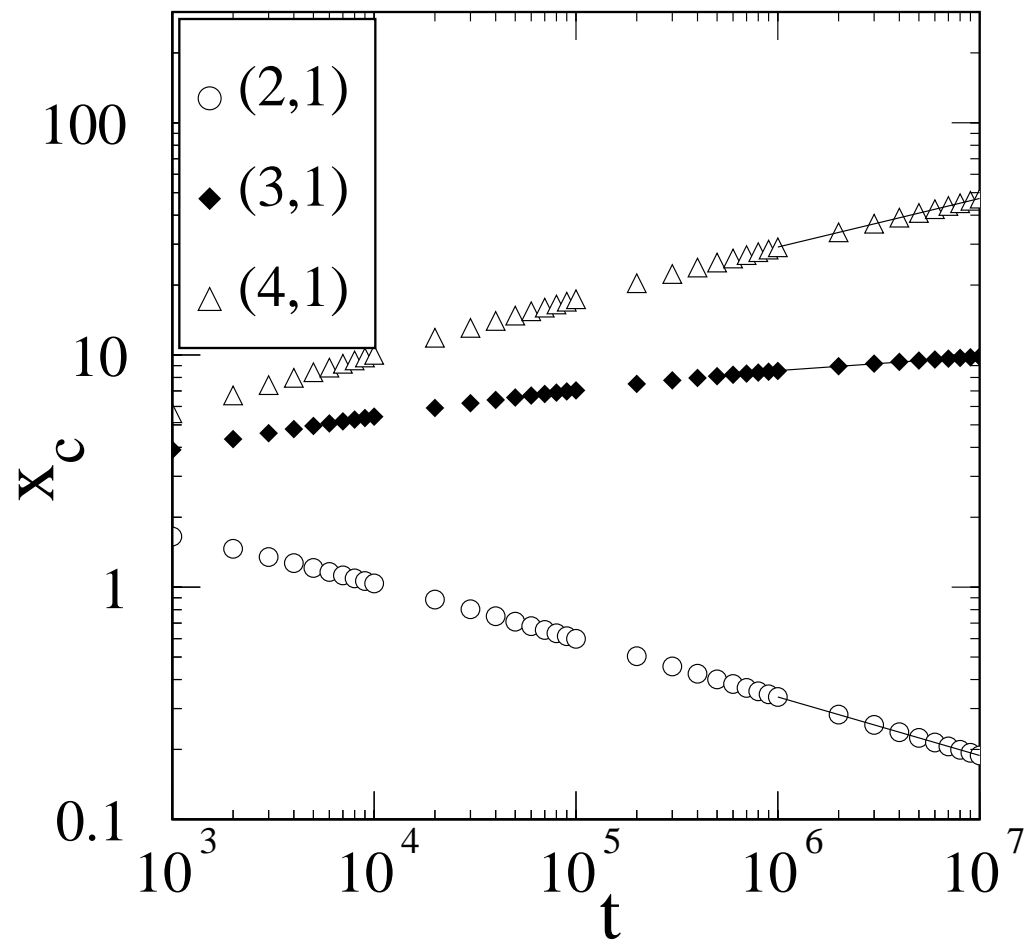


Figure 7